Journal of Visualization, Vol. 3, No. 4 (2001) 331-339

Khan, M. U.*[1], Hirahara, H.*[2] and Kawahashi, M.*[2]

*1 Graduate School of Science and Engineering, Saitama University, 255 Shimo-Okubo, Urawa, Saitama 338-8570, Japan.
*2 Faculty of Engineering, Saitama University, 255 Shimo-Okubo, Urawa, Saitama 338-8570, Japan.

Received 11 September 2000.
Revised 17 November 2000.

***Abstract*:** Flows over a two-dimensional rectangular cavity, which length to depth ratios are 1 and 2, were studied experimentally and numerically at Mach numbers, 0.55 to 0.85. The flow pattern and unsteady wave propagation were visualized by using a schlieren technique. The pressure fluctuation in the cavity was analyzed by FFT. Its spectrum distribution was discussed for several flow Mach numbers. The experimental results were compared with the previous theory in terms of the discrete frequencies. Comparing experimental results and those theoretical predictions, oscillation modes in transverse and longitudinal directions were discussed with visualized flow images. A numerical simulation was carried out by a finite difference method at a free stream Mach number of 0.8. The numerical simulation demonstrated the periodic formation of the vortices at the leading edge and shedding to the trailing edge. A comparison of the numerical result with experimental observation shows a good agreement in terms of flow pattern in the cavity.

***Keywords*:** subsonic and transonic cavity flow, sound emission, schlieren technique.

Sound emission from cavity, jet or body submerged in a flow, is a very important problem in fluid mechanics or aerodynamics. In generel, cavity flow, jet flow and other similar flows might accompany a discrete sound emission. A study of these phenomena is very important because sound emission from a cavity is one of the basic problems in noise generation and occurs in many practical applications e.g. slotted walls, duct or pipe joints in industrial facilities, airplanes, automobiles and other vehicles, etc. These phenomena associated with flow-induced noise and acoustic oscillations in cavity have been investigated by many researchers in the past. Plumblee et al. (1962), Norton (1952), Owen (1958) and Krishnamurty (1955) have studied the acoustic resonance and noise emission in the cavity flow. Krishnamurty (1955) found that cavity flow might oscillate under a broad band of flow condition in a supersonic flow regime. Rossiter (1964) presented the feedback mechanism, which was able to explain the flow oscillation mechanism. Heller et al. (1971) improved the Rossiter's empirical formula assuming sound speed in the cavity equals to the stagnation sound speed in free stream. Tam and Block (1978) developed a linearized theory to take account the features of the shear layer instability and the impingement of the shear layer near the trailing edge. They investigated the low speed cavity flow and obtained a good agreement with experimental data. Recently, Zhang and Edwards (1990) studied the oscillation types in a supersonic cavity flow. According to Zhang, the longitudinal oscillation is characterized by a large unstable trailing edge vortex and vortices shed from the leading edge of cavity. On the other hand, the behavior of a trailing edge vortex in the cavity characterized the transverse oscillation. They pointed out that the trailing edge vortex was very important to sustain the oscillation. Tracy et al. (1992) investigated the transonic cavity flow at L/D ratio from 4.00 to 20.00.

They observed that mode and bandwidth depended on the Mach number. Bilanin and Covert (1993) modeled the physical process which sustained discrete-frequency oscillations of cavities in compressible flow. A formula that predicts excitation frequencies as a function of Mach number and cavity geometry was discussed in his report. Sakamoto et al. (1995) investigated a longer cavity flow, in which three-dimensional vortices structure was discussed. Takakura et al. (1995,1996) also investigated a three-dimensional flow of the shear layer numerically. Rizzetta (1988) found details of the flow field structure, which was elucidated by solving averaged Navier-Stokes equations. He verified that the behavior of these phenomena was basically two-dimensional.

As described above, in order to investigate sound resonance phenomena, three factors are important. First factor is the vortex shedding from a leading edge. The thickness and turbulence of incoming boundary layer influenced on the instability of a shear layer, which was separated from the leading edge. Second important factor is the determination of the sound source near the trailing edge. The estimation of the sound intensity as the sound source is very difficult but essential in this field. The last factor is the detection of sound feedback path on the resonance. Depending on a flow Mach number, the feedback path might be changed and various oscillation modes will be established. In the present paper, flow visualization was performed in order to investigate these oscillation mechanisms. It is expected to give us important information about the resonant mechanism in the cavity. Then, vortex shedding and instability of shear layer were studied by the visualization. The mode of flow oscillation was discussed by the pressure fluctuation measurement and the mechanism of the sound emission was discussed in terms of the mode.

Experiment was carried out with an intermittent wind tunnel. Schematic diagram of the experimental set-up was shown in Fig. 1. The cross section and span of the channel were $25 \times 20\text{mm}^2$ and 25mm. Depth of the cavity D was kept constant, 20mm. The longitudinal lengths of the cavity L were 20 and 40mm when L/D = 1 and 2 respectively. By changing the throat height, which was located downstream of the test section, Mach number of free stream was varied from 0.55 to 0.85 (see Fig. 1(b)). The vacuum tank was connected with the test section and the initial pressure of the test section was at atmospheric pressure. The volume of the vacuum tank was 0.79m^3 and the time duration for the experiment was approximately 2 sec. Evacuating the vacuum tank to 10 Torr, the diaphragm was broken to make the flow start. The test section and the vacuum tank were separated by a

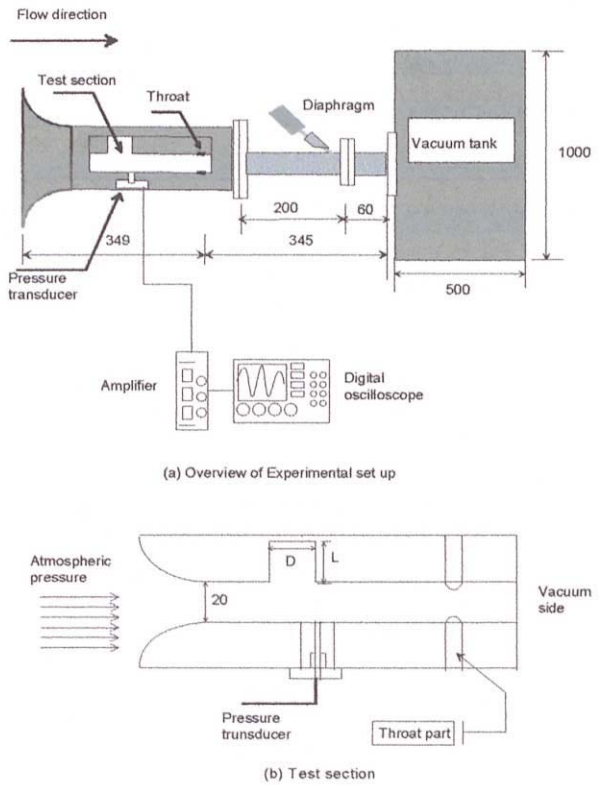

Fig. 1. Experimental set up.

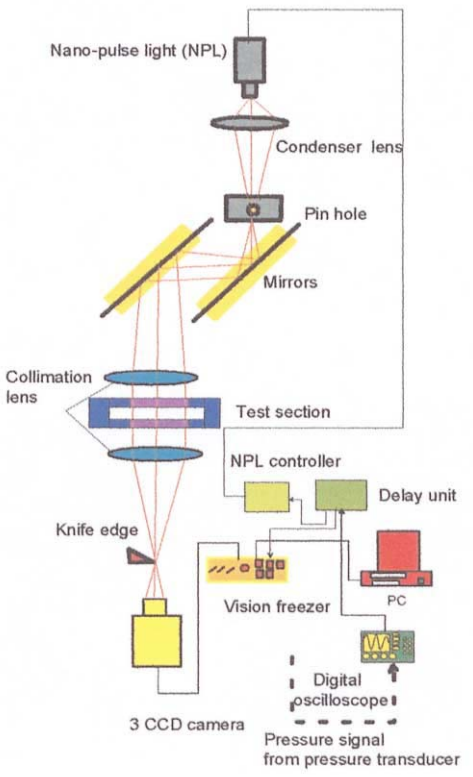

Fig. 2. Optical system.

diaphragm which was 50 micrometer thick. After breaking the diaphragm, flow started. The flush mounted semi-conductor transducer (Kulite XCQ-062-50A) was used to measure the pressure in the test section. Location of the pressure transducer was shown in Fig. 1. Pressure signal was recorded by a digital strage oscilloscope (YOKOGAWA DL4100). Sampling rate of the pressure signal was 100kHz. The power spectrum density was obtained by processing the pressure signal with FFT on PC.

Flow visualization was carried out by a schlieren method as shown in Fig. 2. A nano-pulse light was used as a light source for the flow visualization. The duration of flush light was 180nsec. A delay unit was also used to capture the images at any instant time. Instantaneous pressure signal from digital oscilloscope via amplifier was used as input signal for the delay unit. The outputs of the delay unit were used to illuminate the nano-pulse light and to control the shutter of 3CCD camera (Sony XC-003). Experiments were carried out for two cavity configuration, $L/D = 1$ (case-1) and $L/D = 2$ (case-2). The cavity configuration $L/D = 1$ is typical one, however, it is difficult to distinguish the difference between a longitudinal mode and a transverse mode. Case-2 was tested for comparing these modes.

Since the amplitude of the propagating sound wave may be less than a several kPa and the width of the test section is only 20mm, it is difficult to visualize the flow under the present condition. In order to visualize a propagating sound wave in the free stream and in the cavity, the optical arrangement was tuned up with special attention.

Numerical simulation was carried out by solving a set of mass conservation equation, two-dimensional compressible Navier-Stokes equations and energy equation. A MUSCL-TVD scheme was employed in the present simulation, which was developed by Yee (1986). The scheme has third order accuracy in space and second order in time. An orthogonal fine mesh (400×300) was used to establish a high spatial resolution. The conservation form of governing equation for a viscous compressible flow is expressed in the following form.

$$\frac{\partial U}{\partial t} + \frac{\partial E}{\partial x} + \frac{\partial F}{\partial y} = \frac{1}{\mathrm{Re}} \left(\frac{\partial R}{\partial x} + \frac{\partial S}{\partial y} \right) \tag{1}$$

As the initial condition, the flow is taken to be uniform behind the leading edge of the cavity. The values of the simulation parameters are shown in Table 1.

$$E = \begin{bmatrix} \rho u \\ \rho u^2 + p \\ \rho uv \\ (e+p)u \end{bmatrix} \quad F = \begin{bmatrix} \rho m^{v} \\ \rho m^{vu} \\ \rho m^{v^2} + p \\ (e+p)^{v} \end{bmatrix} \quad R = \begin{bmatrix} 0 \\ \tau_{xx} \\ \tau_{xy} \\ u\tau_{xx} + v\tau_{yx} + q_x \end{bmatrix} \quad S = \begin{bmatrix} 0 \\ \tau_{xy} \\ \tau_{yy} \\ u\tau_{xy} + v\tau_{yy} + q_y \end{bmatrix}$$

Here, ρ is the density, u and v are the velocity components of the flow, p is pressure, e is the specific energy, τ_{xx}, τ_{xy} and τ_{yy} are the components of stress tensor and q_x and q_y are the x and y components of the heat flux.

Table 1. Parameter used in the simulation.

Parameter	Initial value
Free stream pressure	52.8 kPa
Free stream temperature	200 K
Sound speed in free stream	283.8 m/s
Mach number	0.8325
Prandtl number	0.714
CFL number	0.1
Entropy correction parameter	0.001
Artificial compression parameter	0.50

4.1 Flow Visualization

Flow visualization was carried out to clarify the flow mechanism. This is very effective for understanding the sound emission process. To synchronize the photo-capturing time with a phase of flow oscillation is very difficult in the current system. So, the photograph was taken at instant time after the flow starting. Figure 3 shows schlieren photographs of the cavity with vertical knife-edge (case-1) where horizontal density gradiation is visible. The images are taken at t_d = 5, 30, 300, 500msec. It was recognized from the pressure record that a sound emission had been started after 5ms. At t_d = 5ms, a vortex is just formed at the leading edge, and another vortex is already reached up to the trailing edge. In the next figure (t_d = 30msec) a vortex is already formed and it moves from the leading edge. At this moment, the trailing edge vortex becomes larger. At t_d = 300msec, an oncoming vortex in the shear layer almost reaches the trailing edge. At this moment, the trailing edge vortex becomes weaker. Figure 3(d) is almost similar to Fig. 3(a). According to the recorded pressure data, the dominant frequency was 8kHz, therefore 125 sec is necessary to complete one cycle of the oscillation. Unfortunately, it is impossible to visualize the flow with such short time steps with the present apparatus. For this reason, we captured as many as 70 images within the experiment duration of 2sec. After analyzing these images, finally we present the above oscillation cycle. According to such manner, it was found that an encounter of the vortices on the trailing edge was observed and it induced the instability of shear layer. In these photographs, propagating sound waves were visualized. It is shown that sound waves propagate periodically in a main stream beyond the cavity. It seems that these sound waves were generated at the trailing edge when the vortices encountered on it. This is a well known fact in the previous studies and is reasonable. However, the propagating wave inside the cavity is hard to recognize from these photographs. In order to study the wave propagation inside the cavity, we require a more precise and repeated observation. If we take a correlation in terms of the density gradient between these flow images, it will be possible to clear the sound propagation in the cavity. It is important to know whether the sound waves propagating in a main stream is dominant or the sound waves propagating inside a cavity. Further detailed inspection should be carried out with a high-speed video camera.

Figure 4 shows schlieren photographs (at t_d = 700msec) of the cavity with horizontal knife-edge setting for the case-1 and case-2. In this setting, vertical density gradient was visualized, so the boundary layer thickness and width of the shear layer were recognized qualitatively. In this figure, for case-1, an incoming boundary layer and the shear layer spanning the cavity were visualized clearly. It is found that the shear layer deflection in the case of L/D = 1 was smaller than in the case of L/D = 2.

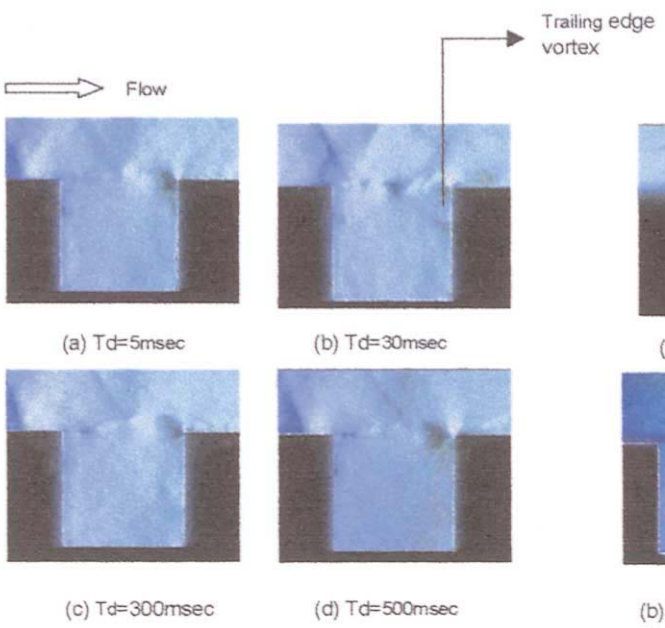

Fig. 3. Schlieren photographs (knife-edge vertical, L/D = 1).

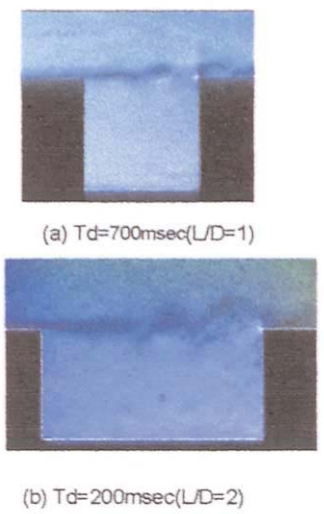

Fig. 4. Schlieren photographs (knife-edge horizontal).

4.2 Influence of Flow Mach Number on the Power Spectrum

From the results in FFT analysis, four discrete frequencies were found explicitly. The peak values of power spectrum density (PSD) for discrete frequencies of 1st, 2nd, 3rd and 4th are plotted in Fig. 5. For the case-1 (L/D = 1), a pressure amplitude at the second oscillatory frequency becomes superior when the flow Mach number is greater than 0.65. When the flow Mach number is in the range from 0.6 to 0.65, the 3rd discrete frequency becomes dominant. After that it gradually decreases. In case-2 (L/D = 2), the spurious frequency in PSD was second discrete frequency throughout the entire Mach number range. In the next section, these oscillation frequencies will be discussed. PSD data were scattered in both cases. Especially, in L/D = 1, they are more scattered than in L/D = 2. The reason for this type of scattering is not clear at the moment. The absolute value of PSD might be very sensitive for the initial condition.

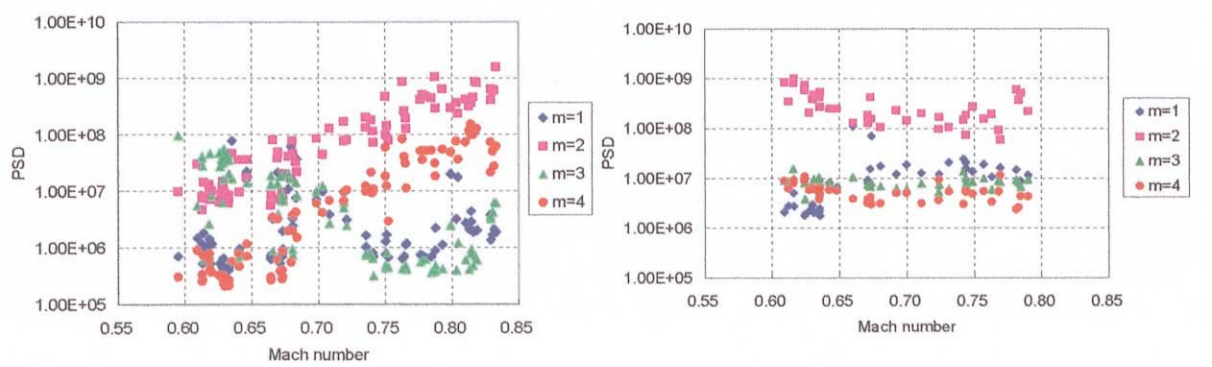

(a) L/D=1 (b) L/D=2

Fig. 5. Effects of Mach number on the power spectrum density.

4.3 Oscillatory Frequency

Figure 6 shows the comparison between the longitudinal and the transverse oscillatory modes with the experimental data. The solid lines show the predicted oscillatory mode frequency and the symbols correspond to the experimental frequency. According to the standing wave approximation for the transverse oscillatory mode, the frequency will be predicted by the following equation.

$$f_{mt} = \frac{na_c}{4L_c} \qquad n = 1, 2, 3, \ldots \tag{2}$$

Here, a_c is the sound speed in the cavity and L_c is the characteristic length of the cavity. Now, L_c is taken as the depth of the cavity. Figure 6(a) shows a fair agreement between the experimental data and the oscillatory frequency predicted by Eq. (2). So, cavity flow may oscillate in the transverse mode for L/D = 1.

Now, if the longitudinal mode of the standing wave is considered, the frequency will be predicted by the following equation.

$$f_{ml} = \frac{na_c}{2L_c} \qquad n = 1, 2, 3, \ldots \tag{3}$$

The characteristic length L_c for longitudinal mode is taken as the length of the cavity. The first oscillatory mode of the standing wave was found at the second oscillatory frequency of the experiments but the third oscillatory frequency of the experiments was unable to predict by the standing wave theory (Fig.6(b)). Therefore, longitudinal oscillatory mode of the standing wave did not agree with the experimental data. Although the transverse oscillation might be dominant at L/D = 1, the oscillation mechanism should be more complicated one. The major question is the mechanism of sound source excitation. The excitation mechanism is quite different in L/D = 1 and 2. For the longitudinal mode, a solid boundary reflection condition should be assigned at the leading edge, and the shear layer should be disturbed in longitudinal direction. Under this condition, the shear layer should be stretched in flow direction. On the other hand, for transverse mode, a free boundary condition should be assigned at the leading edge. In this case, the shear layer is disturbed in transverse direction so that it should be influenced by a

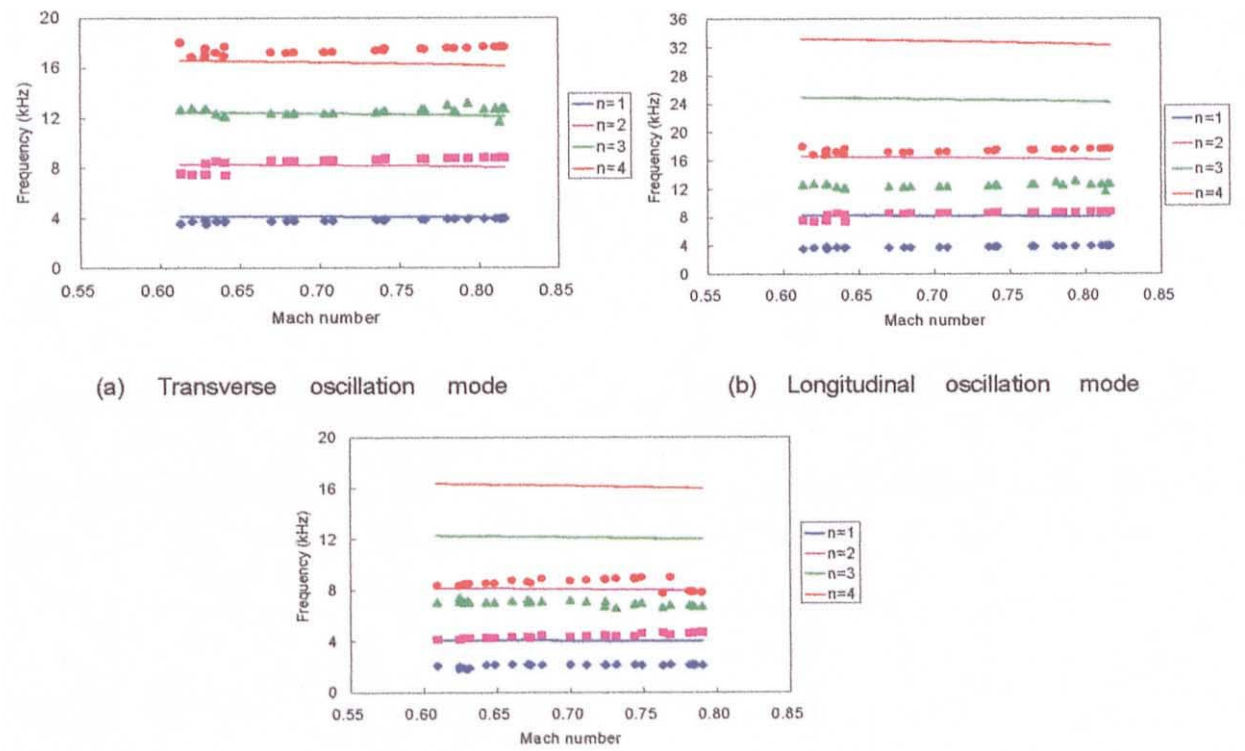

Fig. 6. Comparison of standing wave theory with experimental.

vertical convection force. In the case-1, although it is reasonably found that the transverse oscillation is dominant, it should be considered that the flow is influenced by transverse oscillation and longitudinal oscillation and consequently they are coupled.

For the case-2, let L_c be cavity depth in Eq. (2) and L_c be cavity length in Eq. (3), then the frequencies of longitudinal and transverse mode become equal. The first oscillatory frequency of the longitudinal mode agrees fairly with the second oscillatory frequency of the experiment throughout the entire Mach number range (Fig.6(c)). From the optical observation, it is concluded that the cavity may oscillate in either longitudinal or transverse oscillatory mode.

Rossiter (1964) discussed the fundamental oscillation mechanism in his report. According to the feedback mechanism by Rossiter, the frequency of the periodic pressure fluctuation was expressed by the following equation.

$$f = \frac{U_e}{L}\frac{m-\boldsymbol{a}}{M+1/K_c} \qquad m=1,2,3,... \tag{4}$$

Here $\boldsymbol{a}$ is an empirical parameter for phase shift between the vortices and pressure waves, M, U_e and L are Mach numbers, free stream velocity and length of the cavity respectively. K_c is the ratio between the free stream velocity and the convection speed of vortices in the shear layer. Heller et al. (1971) improved the Rossiter's empirical formula by assuming the sound speed in the cavity equals to the stagnation sound speed in free stream.

$$f = \frac{U_e}{L}\frac{m-\boldsymbol{a}}{M/\sqrt{1+1/2(k-1)M^2}+1/K_c} \qquad m=1,2,3,... \tag{5}$$

Here, $\boldsymbol{K}$ is the specific heat ratio.

The experimental results of the discrete frequency at different Mach numbers for the case-1 and case-2 are shown in the Fig. 7. The solid lines show the experimental frequencies, which were at the same stage of the predicted frequencies by Eq. (5). The discrete frequencies for the case-1 become almost half for the case-2. The spurious discrete frequencies were shown by solid rectangles. At L/D = 1, the dominant frequency 'jumps' from one mode to another mode. This jump occurs at Mach number 0.65. However, such a jump was not observed in case-2 discussed in the above, where the oscillation always took place in the same mode.

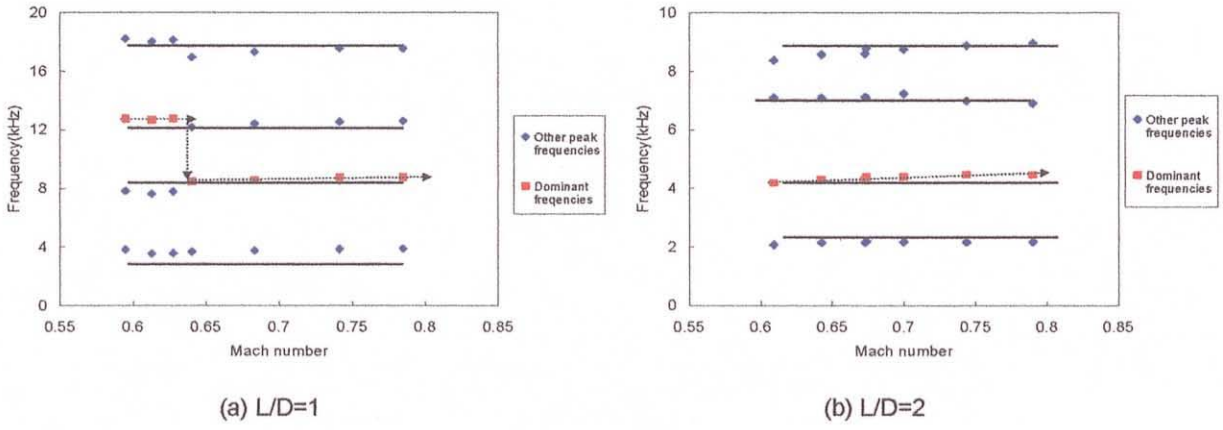

Fig. 7. Frequencies of pressure fluctuation in the cavity.

4.4 Numerical Results

Figure 8 shows the velocity vectors diagram after the self-sustained oscillation started. The vortices shedding from the leading edge was observed. When the flow interacts with the trailing edge of the cavity, a large trailing edge vortex was appeared in the cavity. After that, this trailing edge vortex moves in the transverse direction. The formation of the vortex requires much time and it gradually becomes strong. When it becomes sufficiently strong, it travels at a higher speed. In this manner, the leading edge vortex reaches to the trailing edge of the cavity. At this moment, the trailing edge vortex, which is pushed toward the bottom of the cavity by the shear layer is accompanied by the arrival of the leading edge vortex. After mixing with the new vortices, the first vortex becomes strong. Then another leading edge vortex appears in the shear layer. During this process, the trailing edge vortex becomes stronger with the mixing. The movement of the first trailing edge vortex was observed in the schlieren observation (Fig. 3). At t = 112.3 (where t is the dimensionless time), the first trailing edge vortex started to shed from the rear face of the cavity. At t = 164.38, the first trailing edge vortex is totally detached from the rear face of the cavity. Zhang and Edwards (1988) also discussed these characteristics of vortex shedding, which were found clearly when the cavity flow oscillates in the longitudinal direction. He also discussed the behavior of vortex in the cavity when the cavity flow oscillates in the transverse direction at supersonic speed. Although our experiment was performed at transonic region, the experimental frequency agreed well with the predicted frequency by the standing wave theory for the transverse direction. Comparing these results and the flow visualization, it can be concluded that cavity flows are strongly influenced by the transverse mode when L/D is 1.

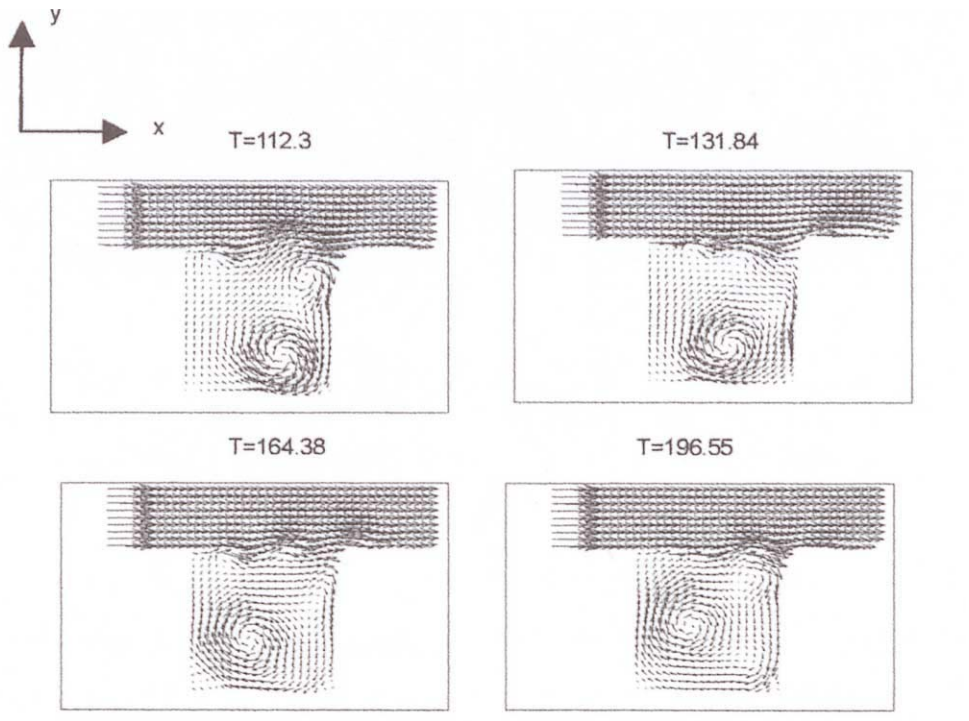

Fig. 8. Velocity vector diagram.

Flow oscillation in the cavity was studied for length to depth ratios of L/D = 1 and 2. The oscillation cycle, vortices shedding and the movement of the trailing edge vortex were observed by the flow visualization. The power spectrum density was measured and its distribution was obtained for a different flow Mach number.

1) When L/D = 1, two oscillatory modes are dominant at two different Mach number ranges. This result indicates that two types of flow oscillation occur in this cavity dimensions. When L/D = 2 only one oscillatory mode is dominant throughout the entire Mach number range. When L/D = 1, experimental frequencies of the different oscillatory modes agree well with the frequencies which were predicted by the standing wave theory for the transverse oscillation. This means that the cavity flow is influenced by the transverse oscillation strongly. When L/D = 2, frequencies which were predicted by the standing wave theory for transverse and longitudinal oscillations did not agree with the experimental frequencies. It means the standing wave theory fails to predict the type of oscillation in this dimension of the cavity.

2) The dominant frequencies jump from one oscillatory mode to another mode between Mach numbers 0.6 to 0.7 when L/D = 1. So, this jump also indicates that there are two types of flow pattern in the different Mach number ranges in this cavity dimension. On the other hand, when L/D = 2 there are no such jumps occurred. It means only one type of flow pattern exists throughout the Mach number range.

3) Periodic vortices shedding and the movement of the trailing edge vortex were observed by the numerical simulation at L/D = 1. The movement of the large single vortex in the middle of the cavity was also observed.

References

Bilanin, A. J. and Covert, E. E., Estimation of possible excitation frequencies for shallow rectangular cavities, AIAA journal, 11-3 (1993), 347-351.

Heller, H. H., Holmes, D. G. and Covert, E. E., Flow-induced pressure oscillation in shallow cavities, Journal of sound and Vibration, 18-4 (1971), 545-553.

Krishnamurty, K., Acoustic radiation from two-dimensional rectangular cutouts in aerodynamic surfaces, NACA, Tech.Note 3487(1955), 1-33.

Norton, D. A., Investigation of B47 bomb bay buffet, Boeing Airplane Co., Document No. D12675 (1952).

Owen, T. W., Techniques of pressure-fluctuation measurements employed in the R.A.E low speed wind tunnels, AGARD Report 172. ARC. 20 780 (1958).

Plumblee, H. E., Gibson, J. S. and Las, L. W., A theoretical and experimental investigation of the acoustic response of cavities in an aerodynamic flow, WADD TR-61-75 (1962).

Rizzetta, D. P., Numerical simulation of supersonic flow over a three-dimensional cavity, AIAA Journal, 26-7 (1988), 799-807.

Rossiter, J. E., Wind-tunnel experiment of the flow over rectangular cavities at subsonic and transonic speeds, British ARCR & M. No.3438 (1964), 1-32.

Sakamoto, K. Matsunaga, K., Fujii, K. and Tamura, Y., Experimental investigation of supersonic internal cavity flow, AIAA paper-95- 2213 (1995), 1-11.

Takakura, Y., Higashino, F.,Yoshizawa, Yoshida, T. M. and Ogawa, S., Parallel computation of unsteady supersonic cavity flows, invited paper, Parallel Computational Fluid dynamics, (1995), 59-66, Elsevier Science Pub.

Takakura, Y., Higashino, F., Yoshizawa, T. and Ogawa, S., Numerical study on unsteady supersonic cavity flows, AIAA paper (1996), 1-9.

Tam, C. K. W. and Block P. J. W., On the tones and pressure oscillations induced by flow over rectangular cavities, J. Fluid Mech., 89-2 (1978), 373-399.

Tracy, T. B., Plentovich, E. B. and Chu, J., Measurements of fluctuating pressures in a rectangular cavity in transonic flow at high Reynolds number, NASA Technical Memorandum 4363 (1992), 1-29.

Yee, H. C., Linearized form of implicit TVD schemes for the multidimensional Euler and Navier-Stokes equation, Comp. & Maths. with Appls., 12A-4/5 (1986), 413-432.

Zhang, X. and Edwards, J. A., Computational analysis of unsteady supersonic cavity flows driven by thick shear layers, Aeronaut, 92-919 (1988), 364-375.

Zhang, X. and Edwards, J. A., An investigation of supersonic oscillatory cavity flows driven by thick shear layers, Aeronaut J. December, (1990), 355-365.

Author Profile

Maksud Uddin Khan: He received his Masters Degree in Mechanical Engineering from Saitama University in 2000. Now he is doing Ph.D. in the same University.

Hiroyuki Hirahara: He received his Master of Mechanical Engineering degree in 1983, and his D. Eng. degree in 1986 in Khyushu University. After the D. Eng. course, he worked in atomic power plant engineering section in Toshiba Co. Ltd. He worked as a Research Assistant and a Lecturer of Saitama University, before taking up his current position. He is an Associate Professor of Saitama University, and his research subjects are high speed flow, supersonic flow with condensation or evaporation, flow measuring techniques, optical measurement techniques and environmental fluid mechanics.

Masaaki Kawahashi: He received his MSc(Eng) degree in 1968 from University of Electro-Communication, and his D.Eng. in 1978 from the University of Tokyo. After MSc he worked as a Research Assitant, a Lecturer and an Associate Professor at Saitama University before taking up his current position as a Professor at Saitama University. His research interests are in thermo-fluid phenomena by finite amplitude wave motion in ducts, speckle metrology and PIV measurement of complicated flow fields in centrifugal fan.